Defense Threat Reduction Agency
8725 John J. Kingman Road, MS
6201 Fort Belvoir, VA 22060-6201

DTRA-TR-15-19

TECHNICAL REPORT

Development of a Guinea Pig Lung Deposition Model

January 2016

DTRA01-03-D-0014

Bahman Asgharian

Prepared by:
Applied Research Associates, Inc.
801 N. Quincy Street
Suite 700
Arlington, VA 22203

DESTRUCTION NOTICE:

Destroy this report when it is no longer needed.
Do not return to sender.

PLEASE NOTIFY THE DEFENSE THREAT REDUCTION AGENCY, ATTN: DTRIAC/ J9STT, 8725 JOHN J. KINGMAN ROAD, MS-6201, FT BELVOIR, VA 22060-6201, IF YOUR ADDRESS IS INCORRECT, IF YOU WISH IT DELETED FROM THE DISTRIBUTION LIST, OR IF THE ADDRESSEE IS NO LONGER EMPLOYED BY YOUR ORGANIZATION.

REPORT DOCUMENTATION PAGE

Form Approved
OMB No. 0704-0188

1. REPORT DATE *(DD-MM-YYYY)*	**2. REPORT TYPE**	**3. DATES COVERED** *(From - To)*
00-01-2016	Technical	February 10, 2011 - January 10, 2012

4. TITLE AND SUBTITLE

Development of a Guinea Pig Lung Deposition Model

5a. CONTRACT NUMBER

DTRA01-03-D-0014-0030

5b. GRANT NUMBER

5c. PROGRAM ELEMENT NUMBER

6. AUTHOR(S)

Bahman Asgharian

5d. PROJECT NUMBER

5e. TASK NUMBER

5f. WORK UNIT NUMBER

7. PERFORMING ORGANIZATION NAME(S) AND ADDRESS(ES)

Applied Research Associates, Inc.
801 N. Quincy St., Suite 700
Arlington, VA 22203

8. PERFORMING ORGANIZATION REPORT NUMBER

9. SPONSORING / MONITORING AGENCY NAME(S) AND ADDRESS(ES)

Defense Threat Reduction Agency
8725 John J. Kingman Road, STOP 6201
Fort Belvoir, VA 22060-6201

10. SPONSOR/MONITOR'S ACRONYM(S)

DTRA

11. SPONSOR/MONITOR'S REPORT NUMBER(S)

DTRA-TR-15-19

12. DISTRIBUTION / AVAILABILITY STATEMENT

Distribution Statement A. Approved for public release; distribution is unlimited.

13. SUPPLEMENTARY NOTES

This work was sponsored by the Defense Threat Reduction Agency.

14. ABSTRACT

Guinea pigs have been used as a surrogate for humans in a number of inhalation toxicology studies by exposing the animals to airborne viruses, biological agents, and other chemicals. Findings from these studies can be extrapolated to humans based on a particular dose-metric of interest to determine potential health effects in humans. In the absence of exposure-dose data, mathematical models can be developed for the transport and deposition of inhaled particles in the lungs of guinea pigs to allow for predictions of lobar, regional, and local deposition of particles.

15. SUBJECT TERMS

MPPD Guinea Pig Particle Deposition respiratory

16. SECURITY CLASSIFICATION OF:			**17. LIMITATION OF ABSTRACT**	**18. NUMBER OF PAGES**	**19a. NAME OF RESPONSIBLE PERSON**
a. REPORT	**b. ABSTRACT**	**c. THIS PAGE**	SAR	23	Richard Fry
Unclassified	Unclassified	Unclassified			**19b. TELEPHONE NUMBER** *(include area code)* 703-767-3193

UNIT CONVERSION TABLE

U.S. customary units to and from international units of measurement*

U.S. Customary Units	Multiply by → / ← Divide by†		International Units
Length/Area/Volume			
inch (in)	2.54	$\times 10^{-2}$	meter (m)
foot (ft)	3.048	$\times 10^{-1}$	meter (m)
yard (yd)	9.144	$\times 10^{-1}$	meter (m)
mile (mi, international)	1.609 344	$\times 10^{3}$	meter (m)
mile (nmi, nautical, U.S.)	1.852	$\times 10^{3}$	meter (m)
barn (b)	1	$\times 10^{-28}$	square meter (m^2)
gallon (gal, U.S. liquid)	3.785 412	$\times 10^{-3}$	cubic meter (m^3)
cubic foot (ft^3)	2.831 685	$\times 10^{-2}$	cubic meter (m^3)
Mass/Density			
pound (lb)	4.535 924	$\times 10^{-1}$	kilogram (kg)
unified atomic mass unit (amu)	1.660 539	$\times 10^{-27}$	kilogram (kg)
pound-mass per cubic foot (lb ft^{-3})	1.601 846	$\times 10^{1}$	kilogram per cubic meter (kg m^{-3})
pound-force (lbf avoirdupois)	4.448 222		newton (N)
Energy/Work/Power			
electron volt (eV)	1.602 177	$\times 10^{-19}$	joule (J)
erg	1	$\times 10^{-7}$	joule (J)
kiloton (kt) (TNT equivalent)	4.184	$\times 10^{12}$	joule (J)
British thermal unit (Btu) (thermochemical)	1.054 350	$\times 10^{3}$	joule (J)
foot-pound-force (ft lbf)	1.355 818		joule (J)
calorie (cal) (thermochemical)	4.184		joule (J)
Pressure			
atmosphere (atm)	1.013 250	$\times 10^{5}$	pascal (Pa)
pound force per square inch (psi)	6.984 757	$\times 10^{3}$	pascal (Pa)
Temperature			
degree Fahrenheit (^oF)	$[T(^oF) - 32]/1.8$		degree Celsius (^oC)
degree Fahrenheit (^oF)	$[T(^oF) + 459.67]/1.8$		kelvin (K)
Radiation			
curie (Ci) [activity of radionuclides]	3.7	$\times 10^{10}$	per second (s^{-1}) [becquerel (Bq)]
roentgen (R) [air exposure]	2.579 760	$\times 10^{-4}$	coulomb per kilogram (C kg^{-1})
rad [absorbed dose]	1	$\times 10^{-2}$	joule per kilogram (J kg^{-1}) [gray (Gy)]
rem [equivalent and effective dose]	1	$\times 10^{-2}$	joule per kilogram (J kg^{-1}) [sievert (Sv)]

*Specific details regarding the implementation of SI units may be viewed at http://www.bipm.org/en/si/.

†Multiply the U.S. customary unit by the factor to get the international unit. Divide the international unit by the factor to get the U.S. customary unit.

TABLE OF CONTENTS

LIST OF FIGURES

PREFACE

The research work described in this report was conducted for the Defense Threat Reduction Agency (DTRA) under contract number DTRA01-03-D-0014-0030.

1.0 INTRODUCTION

The guinea pig is a popular animal model to study lung function impairment, asthma, and airway hyper-responsiveness (Hargaden and Singer, 1997). Guinea pigs have been used as a surrogate for humans in a number of inhalation toxicology studies by exposing the animals to airborne viruses, biological agents, and other chemicals (Allon et al., 1998; Botham et al., 1988; Chen et al., 1992; Conner et al., 1988; Fryer et al., 1990; and many others). Findings from these studies can be extrapolated to humans based on a particular dose-metric of interest to determine potential health effects in humans. To investigate dose-dependent biological outcomes for an exposure setting, it is necessary to determine the initial deposition and subsequent fate of inhaled materials in the lungs of guinea pigs. However, little or no data are available on the deposited dose to aid in the construction of an exposure-dose-response relationship. In the absence of exposure-dose data, mathematical models can be developed for the transport and deposition of inhaled particles in the lungs of guinea pigs to allow for predictions of lobar, regional, and local deposition of particles (Anjilvel and Asgharian, 1995). Such models have already been developed for humans, rats, mice, and monkeys (Multiple Path Particle Dosimetry Model, MPPD V2.1, Applied Research Associates; Raleigh, NC; http://www.ara.com/products/mppd.htm). By using species-specific information on lung geometry, and lung and breathing parameters, the deposition model for these species can be extended to guinea pigs.

2.0 MOTIVATION

Mechanistic models for the deposition of particles in the lungs of various species allow linking exposure scenarios to biological responses and interspecies extrapolation for risk analysis. Deposition models, once verified by comparison to measurements, offer a quick and inexpensive alternative to predict lung deposition particularly in cases for which inhalation exposure is either infeasible or lacking. Thus, mechanistically-based particle deposition models are desirable to describe the transport and deposition of inhaled particles in the lungs of guinea pigs. The deposition model used here is based on the multiple-path geometry that was previously developed for humans, rats, mice, and rhesus monkeys (Asgharian *et al*., 2012; Price *et al*., 2002). Inputs to the model include lung geometry and volumes as well as physiological parameters of guinea pigs. Model predictions include deposition fraction and number or mass of the deposited particles per airway generation or region of the lung. Upper and lower limits for deposition predictions are obtained through sensitivity analysis by varying input parameters of the model.

3.0 APPROACH

The approach to calculating particle deposition in the lungs of guinea pigs is similar to that for mice and other species. Detailed fluid dynamics calculations of the airflow or particle transport in lung airways are not feasible due to the large number of airways, complexity of the lung geometry, and lack of data on pleural pressure distribution which provide the necessary outlet boundary conditions to pull the airflow into the lung. Instead, cross-sectional area-averaged mass balance equations for the airflow and particle transport are solved in each airway of the lung starting from the trachea and sequentially moving down the lung airway tree until reaching the most distal airways of the lung. Average deposition fractions of inhaled particles per airway generation and region of the lung are obtained with reasonable accuracy considering variation in deposition due to intersubject variability and uncertainties regarding lung and breathing parameters. The modeling approach involves several steps which are described below in separate sections.

3.1. MODELING DEPOSITION EFFICIENCY IN THE UPPER RESPIRATORY TRACT

Particles deposit in the upper respiratory tract (URT) by two distinct mechanisms: Brownian diffusion for submicrometer particles and inertial impaction for larger particles. There is no information regarding the deposition of submicrometer particles in the URT of guinea pigs either analytically or experimentally. Raabe et al. (1988) conducted a nose-only inhalation exposure in which guinea pigs were exposed to particles ranging from 0.3 μm to about 10 μm in aerodynamic resistance diameter. The exposure duration was limited to only a few minutes to ensure little or no clearance of particles from the airways. Hence, the reported measurements reflected deposition primarily by inertial impaction and included deposited masses of particles in the nasal and lung airways. The exposure atmosphere was also sampled at an available exposure port of the nose-only exposure unit. These measurements were used here to calculate regional deposition fraction of particles by dividing the deposited mass in a given region by the mass of inhaled particles during the inhalation study. For the sake of simplicity without the loss of generality, the respiratory tract was assumed to be split between the URT and lower respiratory tract (LRT) compartments with animals breathing at a steady-state rate. It was further assumed

with reasonable accuracy that URT deposition efficiencies during inhalation and exhalation were similar. Referring to Figure 1, deposition fractions in the head and lung were found from the following relationships

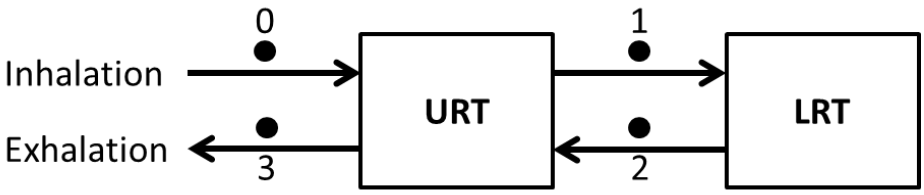

Figure 1. Compartmental representation of the respiratory tract.

$$m_{URT} = m_{in} \times \eta_{URT-imp} + (m_{in} - m_{in} \times \eta_{URT-imp} - m_{LRT}) \times \eta_{URT-imp} \quad (1)$$

in which $\eta_{URT-imp}$ is the deposition efficiency of particles in the URT by impaction during inhalation and exhalation, m_{in} is the mass of inhaled particles and m_{URT}, and m_{LRT} are masses of particles deposited in the URT and LRT, respectively. Dividing both sides of equation (1) by m_{in} and solving for η_{URT} gives

$$\eta_{URT-imp} = \left(1 - \frac{\Delta_{LRT}}{2}\right) - \sqrt{\left(1 - \frac{\Delta_{LRT}}{2}\right)^2 - \Delta_{URT}} \quad (2)$$

In which $\Delta_{URT} = m_{URT} / m_{in}$ and $\Delta_{LRT} = m_{LRT} / m_{in}$ are deposition fractions of particles in the URT and LRT. Measured masses of deposited particles in the URT and LRT from the experiment of Raabe et al. (1988) were used to calculated regional deposition fractions and URT deposition efficiency for each particle size used in the experiment. Calculated URT efficiencies were fit to a logistic function of sigmoidal form to obtain an expression for deposition efficacy by impaction in the URT during inhalation or exhalation as a function of the impaction parameter ($\rho d^2 Q$).

$$\eta_{URT-imp} = \left[1 - \frac{1}{1 + \left(\frac{\rho d^2 Q}{87.909}\right)^{9.976}}\right]^{0.17236} \quad (3)$$

where ρ is the particle mass density, d is the particle diameter, and Q is the inhalation flow rate. The fitted equation explained 98% of the variability in the value of deposition efficiency. Animal

breathing rates and, hence, inhalation/exhalation flow rates were not measured in these experiments. The empirically-based equation of minute ventilation obtained by Guyton (1947) was used to calculate flow rate using the reported weight of the animal by Raabe et al. (1988).

3.2. LUNG GEOMETRY

Measurements of lung airway parameters such as length, diameter, gravity and bifurcation angles are difficult to make due to the enormous amount of airways, irregularity of airway shape, and complexity of lung structure. Measurements were typically made along selected pathways spanning the trachea through the terminal bronchioles of conducting airways. The same measurements were made for the pulmonary airways including respiratory bronchioles, alveolar ducts, and alveolar sacs in the selected paths, which were complemented by measuring the size and number of alveoli per duct. By modeling each airway as a cylindrical tube and the lung as a dichotomous branching network of airways, representative, typical-path, dichotomous and asymmetric lung geometries were constructed for a variety of species (Anjilvel and Asgharian, 1995; Asgharian et al., 2001, 2012).

Information on the lung geometry of guinea pigs is very limited. Early measurements primarily considered the large airways (Tenney and Remmers, 1963; Forrest and Weibel, 1975; Kliment el al., 1972). The most detailed information on guinea pig lung airway dimensions was reported by Schreider and Hutchens (1980). These authors prepared a few lung casts that retained all airways of the lung with diameters of 200 μm and larger. Smaller airways were trimmed off but saved for separate measurements. One cast was completely dissected and airway dimensions were measured. Other casts were partially measured for clarification and to resolve any discrepancies. The completed lung geometry contained 9 generations of conducting airways and 5 generations of respiratory ducts. The lung geometry also included the alveoli, which were distributed fairly evenly among the respiratory ducts. Only measurement of the branching angle was made for the tracheal bifurcation. No measurements of the gravity angle were reported for any of the airways. Thus, an average angle of 45^{o} was chosen for missing angles. The lung geometry of Schreider and Hutchens (1980) was used to calculate particle deposition in the lungs of guinea pigs.

As with other lung geometries in MPPD, airway parameters had to be rescaled twice prior to deposition calculations in guinea pigs: first by $(FRC/TLC)^{1/3}$, where FRC is the functional residual capacity or lung volume at rest and TLC is the total lung capacity, to adjust airway dimensions to rest conditions, and second by $(1+V_T/2)^{1/3}$, where V_T is the tidal volume, to account for airway size change during breathing. The rescaled lung geometry was used in the calculations of particle deposition in the lungs of guinea pigs.

3.3. LUNG VENTILATION AND PHYSIOLOGICAL PARAMETERS

Lung ventilation in guinea pigs follows the same principles as for other rodents. The flow into the lung is created by the difference in pressure between the atmosphere and pleural pressure in the lung cavity during inhalation. While inhalation is initiated by the expansion of the lung cavity to create sub-atmospheric pressure in the pleural space, exhalation is a passive process in which air is let out to allow the pleural pressure to return to equilibrium with the pressure outside of the body. As a result, the airflow is determined by the net effects of lung compliance, airflow inertance, and airway resistance (Asgharian and Price, 2006). Lung expansion and contraction is uniform (each lobe of the lung expands and contracts at a similar rate) in rodents because rodents are typically positioned horizontally. The flow may be assumed to be fully developed (parabolic) because the flow Reynolds number drops to below one after traveling through only a few airway generations. Under such circumstances for uniform lung expansion and contraction, the parent airflow at an airway bifurcation divides in proportion to the distal volume of each daughter airway branch (Yu, 1978). Hence, airflow distribution in lung airways was calculated by traversing down the lung tree and calculating flow rates in daughter branches of an airway bifurcation from the distal-volume proportionality of daughter branches.

There are few measurements of guinea pig respiratory parameters. A review of the available data in the literature was made by Brewer and Cruise (1997). A significant variation was observed among measurements despite the scarcity of the data. North (1999) reported a wide range in breathing frequency between 42 and 150 breaths/min which encompassed reported values of 84 ± 14 breaths/min and 90 (69 – 104) breaths/min by Amdur and Mead (1958) and Guyton (1947), respectively. The tidal volume reported by North (1999) ranged from 1 to 5.3 mL while

Amdur and Mead (1958) and Guyton (1947) reported 1.68 ± 0.39 mL and 1.75 (1 – 3.9) mL, respectively. The volume of the entire nasal cavity was measured by Schreider and Hutchens (1980) to be 0.883 cm^3 which included the sinus and ethmoid area. The nasal cavity alone was measured as $0.483\,cm^3$. There are no reported values for the lung functional residual capacity (FRC). The lung cast made by Schreider and Hutchens (1980) was made at near atmospheric pressure to avoid distorting the chest cavity and edges of the lung. Hence, the measured total lung volume of 21.3 cm^3 by Schreider and Hutchens (1980) was selected as the FRC.

3.4. MECHANISTIC MODEL OF PARTICLE DEPOSITION IN THE LUNG

The particle mass conservation or convective-diffusion equation was developed by accounting for the number of particles that entered, exited, deposited, and remained suspended in an airway per unit time (Anjilvel and Asgharian, 1995; Asgharian et al., 2001; Asgharian and Price, 2007). It was assumed that particle concentration was uniform across the airway cross section but varied with time and location within the airway. First, particle concentration reaching the trachea was calculated by including the filtering effects of the URT by inertial impaction. Next, the convective-diffusion equation was solved in the lung geometry of the guinea pig one airway at a time starting from the trachea and traversing down the lung tree to find particle concentration throughout the lung during inhalation, pause, and exhalation. Particles were carried through lung airways by the airflow generated by a uniform expansion and contraction of lung lobes as described in the previous section. Finally, particle deposition in each airway of the lung was calculated by integrating particle flux over time and airway volume. The deposited fraction of inhaled particles per airway and region of the lung was found by dividing the calculated deposited mass by the mass of inhaled particles. Particle deposition fraction is a unique property for a given lung geometry and set of breathing parameters. Local or regional mass deposited or number of particles deposited was calculated by multiplying the deposition fraction by the mass or number of particles inhaled, respectively.

4.0 SOFTWARE IMPLEMENTATION

We modified the existing MPPD software application to incorporate the guinea pig respiratory deposition models described above. First, the nasal impaction efficiency equation was implemented in the MPPD code. Next, we created geometry data files used to represent the tracheobronchial and pulmonary airway structure in guinea pigs. The files contained airway length, diameter, branching and gravity angle, and alveolar volume (for pulmonary airways) information for each airway generation. The geometry data files were used as input by MPPD to form the tree branching structure within which particle transport and deposition were calculated. Slight modifications to the code were necessary to accommodate the monopodial (instead of the typical dichotomous branching structure) nature of the guinea pig respiratory tract. The lung geometry of Schreider and Hutchens (1979) was used in MPPD as it presents the most complete geometry reported to date. In addition, default respiratory tract volume and breathing parameters were selected from Schreider and Hutchens (1979, 1980), to allow comparison of deposition fractions with theirs. Particle transport and deposition within the guinea pig lung airways was calculated in the same manner as other animal models and implemented as described in the preceding section.

The MPPD graphical user interface (GUI) was modified to accommodate the addition of the guinea pig model. The guinea pig species is an option in the input dialog for animal geometry. Once the model is chosen, respiratory tract volumes (URT, FRC, TLC) and breathing parameters (V_T, breathing frequency, and inspiratory/expiratory fraction) are selected based on Schreider and Hutchens (1979, 1980) as default starting values for the deposition model. These values may be changed at the user's discretion. Once these values are confirmed and the inhaled aerosol characteristics are defined by the user, the model may be executed. Deposition predictions are generated by region (URT, tracheobronchial or TB, pulmonary or PUL, LRT) and also by generation number. Text reports containing a summary of the model predictions and tabulated deposition totals as well as graphical plots of deposition predictions may be generated by the user. These time-stamped reports and plots also contain logs of the input values used for the predictions and may be saved and/or printed for future reference.

5.0 MODEL PREDICITON AND VALIDATION

Regional deposition in the LRT was calculated for guinea pigs for which the lung geometry and physiological parameters were described above. Predictions for regional deposition fractions were made for different particle sizes at a lung tidal volume of $4.44\,cm^3$, breathing frequency of 60 breaths/min., FRC of $21.3\,cm^3$ and nasal volume of $0.68\,cm^3$, which corresponded to the values used in the study by Schreider and Hutchens (1979). Equal inhalation and exhalation time was used with no pause between the two breathing times.

Particle deposition fraction, which is the fraction of inhaled particles that deposits in the lung during a breathing cycle (consisting of inhalation, pause, and exhalation), was calculated for different particle sizes and regions of the lung at the breathing rates and lung volumes stated above. To study the influence of lung physical characteristics in comparison with other species, deposition predictions were made for different particle sizes via endotracheal breathing (i.e., neglecting losses in the nasal passages). Deposition of ultrafine particles (0.01 μm or smaller) in the TB region was quite significant (Figure 2) and as a result, few or no particles reached the PUL region to deposit by Brownian diffusion. As particle size increased, TB deposition decreased and PUL deposition increased. A similar result was observed for fine and coarse particles for which a significant deposition of particles occurred in the TB region by inertial impaction. Particle deposition in the TB region increased with increasing particle size. The TB region served as a filter to reduce penetration of inhaled small and large particles. Consequently, there were two peaks in the PUL curve due to the filtering of particles by the TB region. Overall, total deposition of particles in the LRT was significant for ultrafine and coarse particles due to Brownian diffusion and inertial impaction, respectively. Minimum deposition of particles occurred for particles between 0.5 μm and 1 μm but was still significant at about 10%.

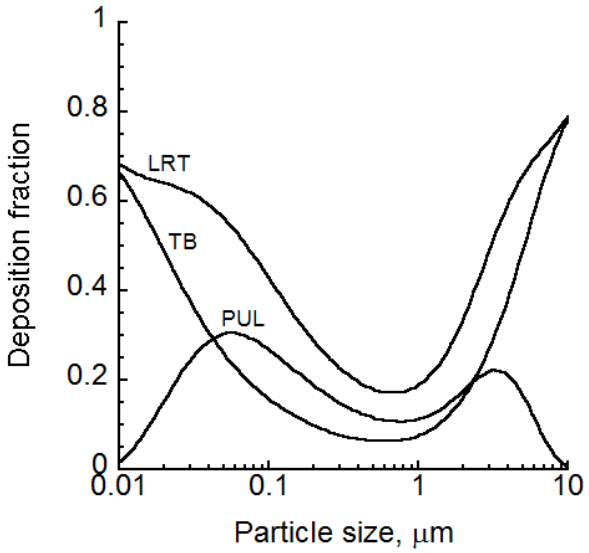

Figure 2. Particle deposition in the lung of the guinea pig via endotracheal breathing.

To study changes in particle deposition with penetration depth of particles, deposition fractions of 0.01, 0.1, 1, and 10 μm particles were calculated in different generations of the guinea pig lung (Figure 3). As a result of strong Brownian diffusion, the majority of 0.01-μm particles deposited in the upper airways of the LRT and, predominantly, in the most distal airway of the TB region. There was little or no particle penetration into the PUL region. Submicrometer particles ranging in diameter between 0.1 and 1 μm showed a relatively small rate of deposition in the TB region and thus reached the PUL region where deposition by Brownian diffusion and gravitational settling occurred. As the size of sub-micrometer particles increased, deposition decreased. Inertial impaction in the TB region increased for particles above 1 μm. As a result, particles were increasingly removed from the inhaled air. For 10-μm particles, deposition occurred entirely in the TB region and mainly in the first few airway generations. There was no penetration of particles into the PUL region. Hence, very small and large particles are primarily filtered out from the inhaled air in the TB region and particles in the intermediate size range (0.1 to 1 μm) are capable of reaching and depositing in the PUL region. These findings have implications in the design of inhalation studies to elicit particle size-dependent, regional biological response in the lungs of guinea pigs.

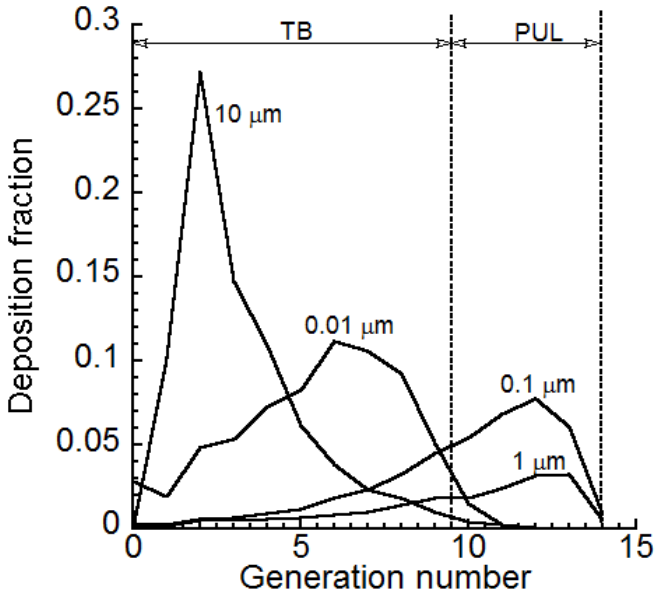

Figure 3. Deposition fraction of various size particles at different lung depths.

Regional deposition fractions of particles with diameters between 0.01 and 10 μm in the respiratory tracts of guinea pigs are given in Figure 4 via nasal breathing for the same physiological parameters stated above. Comparison of predicted deposition fractions in the LRT region via nasal breathing with those for the case of endotracheal breathing (Figure 2) gave similar patterns for submicrometer-sized particles because of the absence of a Brownian diffusion deposition model in the nasal passages. Deposition predictions of fine- and coarse-sized particles regions of the lung were quite different for cases of endotracheal and nasal breathing. Particles larger than 3 μm deposited completely in the nasal passages and as a result there was no penetration or deposition of these particles in the LRT.

Comparison of the predicted regional deposition fraction (Figure 3) in this study with that made by Schreider and Hutchens (1980) given in their Figure 3, showed similar deposition patterns in the TB and PUL regions but size-dependent differences in deposition predictions. Predicted deposition fractions of ultrafine particles by the two models were very similar. Coarse particles were effectively removed in the nasal passages of this study. However, deposition fraction was under 100% in the study by Schreider and Hutchens (1980) and, as a result, there was penetration into the LRT, which decreased with increasing particle size. For intermediate size particles, model predictions from this study gave two distinct peaks of deposition due to the filtering

effects of the nasal and TB airways while predictions of Schreider and Hutchens (1980) showed a fairly uniform deposition in this size range. The difference between the two models stemmed from differences in the predictions of particle deposition in the nasal passages, expressions used to calculate deposition efficiency by each deposition mechanism, and the deposition model: compartmental in Schreider and Hutchens (1980), but mechanistic here capturing anatomical features and structure of the lung, mechanisms of lung breathing, and particle transport.

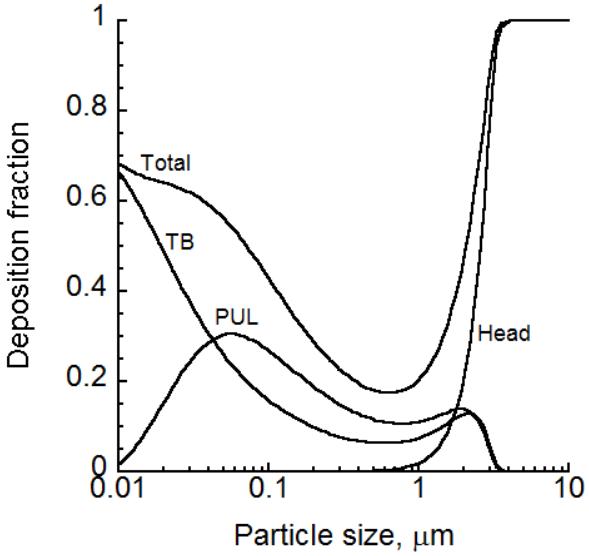

Figure 4. Particle deposition in the lungs of guinea pigs via nasal breathing.

6.0 REFERENCES

Amdur, M.O. and Mead, J. (1958). Mechanics of respiration in unanesthetized guinea pigs. Amer. J. Physiol. 192:364-368.

Anjilvel, S. and Asgharian, B. (1995). A multiple-path model of particle deposition in the rat lung. Fund. Appl. Toxicol. 28:41–50.

Allon, N., Raveh, L., Gilat, E., and Cohen, E. (1998). Prophylaxis against soman inhalation toxicity in guinea pigs by pretreatment alone with human serum butyrylcholinesterase. Toxicological Sciences 43:121-128.

Asgharian, B., Price, O.T., McClellan, G., Corley, R., Daniel R. Einstein, D.R., Richard E. Jacob, R.E., Harkema, J., Carey, S.A., Schelegle, E., Hyde, D., Kimbell, J.S., and Miller, F.J. (2012). Development of a rhesus monkey lung geometry model and application to particle deposition in comparison to humans. Inhalation Toxicology 24:869-899.

Asgharian, B. and Price, O.T. (2007). Deposition of ultrafine (nano) particles in the human lung. Inhalation Toxicology 19:1045-1052.

Asgharian, B. and Price, O.T.,(2006). Airflow distribution in the human lung and its influence on particle deposition. Inhalation Toxicology 18:795-801.

Asgharian, B., Hofmann, W., and Bergmann, R. (2001). Particle deposition in a multiple-path model of human lung. Aerosol Science and Technology 34:332-339.

Botham, P.A., Hext, P.M., Rattray, N.J., Walsh, S.T., and Woodcock, D.R. (1988). Sensitisation of guinea pigs by inhalation exposure to low molecular weight chemicals. Toxicology Letters 41:159-173.

Brewer NR, Cruise LJ. (1997). The Respiratory System of the Guinea Pig: Emphasis on Species Differences. Contemp Top Lab Anim Sci.36:100-108.

Chen, L.C., Fine, J.M., Qu, Q.S., and Amdur, M.O. (1992). Effects of fine and ultrafine sulfuric acid aerosols in guinea pigs: alterations in alveolar macrophage function and intracellular pH. Toxicology and Applied Pharmacology 113:109–117.

Conner, M.W., Flood, W.H., and Rogers, A.E. (1988). Lung injury in guinea pigs caused by multiple exposures to ultrafine zinc oxide: changes in pulmonary lavage fluid. Journal of Toxicology 25:57-69.

Fryer, A.D., E.E., and Jacoby, D.B. (1990). Parainfluenza virus type 1 reduces the affinity of agonists for muscarinic receptors in guinea-pig lung and heart. European Journal of Pharmacology 181:51-58.

Guyton, A.C. (1947). Measurement of respiratory volumes of laboratory animals. Amer. J. Physiol. 15:70-77.

Hargaden, M. and Singer, L. (1997). Anatomy, Physiology, and behavior. In “The Laboratory rabbit, guinea pig, hamster, and other rodents”, (edited by Suckow, M.A., Stevems, K.A., and Wilson, R.P.), Academic Press, Waltham, MA, pp 576-599.

North, D. (1999). The Guinea Pig., In “The UFAW handbook on the Care and management of Laboratory Animals”, seventh ed., (Ed. By Poole, T.), Blackwell Science, LTD, pp. 367-388.

Price, O.T., Asgharian, B., Miller, F.J., Cassee, F.R., and Winter-Sorkina R. de. (2002). Multiple Path Particle Dosimetry Model (MPPD v1.0): A model for human and rat airway particle dosimetry. National Institute for Public Health and the Environment (RIVM) Report 650010030. Bilthoven, the Netherlands.

Raabe, O.G., Al-Bayati, M.A., Teague, S.V., and Rasolt, A. (1988). Regional deposition of inhaled monodisperse coarse and fine aerosol particles in small laboratory animals. Ann. Occup. Hyg. 32 Supplement 1:55-63.

Schreider, J.P., and Hutchens, J.O. (1980). Morphometry of the guinea pig respiratory tract. The Anatomical Record 196:313-321.

Schreider, J.P., and Hutchens, J.O. (1980).Particle deposition in the guinea pig respiratory tract. J. Aerosol Sci. 10:599-607.

Yu, C.P. (1978). Exact analysis of aerosol deposition during steady breathing. Powder Technol. 21:55-62.

DEFINITIONS, ACRONYMS, AND ABBREVIATIONS

ARA	Applied Research Associates, Inc.
DTRA	Defense Threat Reduction Agency
FRC	Functional residual capacity
GUI	Graphical user interface
LRT	Lower respiratory tract
MPPD	Multiple Particle Path Dosimetry
PUL	Pulmonary
TB	Tracheobronchial
TLC	Total lung capacity
URT	Upper respiratory tract

DEPARTMENT OF DEFENSE

DEFENSE TECHNICAL INFORMATION CENTER
8725 JOHN J. KINGMAN ROAD, SUITE 0944
FT. BELVOIR, VA 22060-6218
ATTN: DTIC

QUANTERION SOLUTIONS, INC.
1680 TEXAS STREET, SE
KIRTLAND AFB, NM 87117-5669
ATTN: DTRIAC

JOINT PROJECT MANAGER INFORMATION SYSTEMS (JPM IS)
JOINT PROGRAM EXECUTIVE OFFICE FOR
CHEMICAL BIOLOGICAL DEFENSE (JPEO-CBD)
301 PACIFIC HIGHWAY
SAN DIEGO, CA 92110

DEFENSE THREAT REDUCTION AGENCY
8725 JOHN J. KINGMAN ROAD
FT. BELVOIR, VA 22060-6201
ATTN: DR. CHRISTOPHER KILEY /J9CBA

DEFENSE THREAT REDUCTION AGENCY
8725 JOHN J. KINGMAN ROAD
FT. BELVOIR, VA 22060-6201
ATTN: MR. JERRY GLASOW /J9CBI

DEFENSE THREAT REDUCTION AGENCY
8725 JOHN J. KINGMAN ROAD
FT. BELVOIR, VA 22060-6201
ATTN: MR. RICHARD FRY /J9CBI

DEFENSE THREAT REDUCTION AGENCY
8725 JOHN J. KINGMAN ROAD
FT. BELVOIR, VA 22060-6201
ATTN: MR. THOMAS WOLFINGER /J9CBI

DEFENSE THREAT REDUCTION AGENCY
8725 JOHN J. KINGMAN ROAD
FT. BELVOIR, VA 22060-6201
ATTN: DR. ERIN REICHERT /J9CBM

DEFENSE THREAT REDUCTION AGENCY
8725 JOHN J. KINGMAN ROAD
FT. BELVOIR, VA 22060-6201
ATTN: DR. RON MERIS /J9ISR

DEFENSE THREAT REDUCTION AGENCY
8725 JOHN J. KINGMAN ROAD
FT. BELVOIR, VA 22060-6201
ATTN: DR. AIGUO WU /J9ISR

DEPARTMENT OF DEFENSE CONTRACTORS

APPLIED RESEARCH ASSOCIATES, INC
SECURITY ENGINEERING AND APPLIED SCIENCES
119 MONUMENT PLACE
VICKSBURG, MS 39180-5156
ATTN: MR. JOSEPH L. SMITH